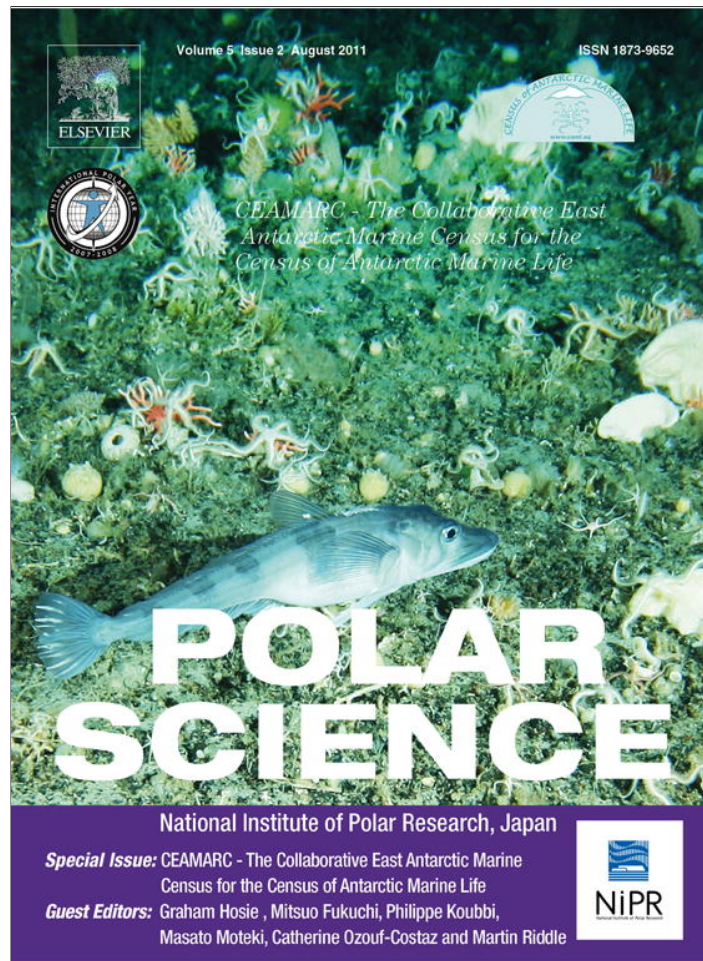


Provided for non-commercial research and education use.
Not for reproduction, distribution or commercial use.



This article appeared in a journal published by Elsevier. The attached copy is furnished to the author for internal non-commercial research and education use, including for instruction at the authors institution and sharing with colleagues.

Other uses, including reproduction and distribution, or selling or licensing copies, or posting to personal, institutional or third party websites are prohibited.

In most cases authors are permitted to post their version of the article (e.g. in Word or Tex form) to their personal website or institutional repository. Authors requiring further information regarding Elsevier's archiving and manuscript policies are encouraged to visit:

<http://www.elsevier.com/copyright>



A GIS approach to estimating interannual variability of sea ice concentration in the Dumont d'Urville Sea near Terre Adélie from 2003 to 2009

Martina B. Smith^{a,b,c,*}, Jean-Philippe Labat^{a,b}, Alexander D. Fraser^d,
 Robert A. Massom^{d,e}, Philippe Koubbi^{a,b}

^a UPMC Université Paris 06, UMR 7093, Laboratoire d'Océanographie de Villefranche, BP28, 06234 Villefranche-sur-Mer, France

^b CNRS, UMR 7093, LOV, BP 28, 06234 Villefranche-sur-Mer, France

^c Spatial Information Science within School of Geography and Environmental Studies, University of Tasmania, Private Bag 76, Hobart, Tasmania 7001, Australia

^d Antarctic Climate and Ecosystems Cooperative Research Centre, University of Tasmania, Private Bag 80, Hobart, Tasmania 7001, Australia

^e Australian Antarctic Division, Department of Sustainability, Environment, Water, Population and Communities, 203 Channel Highway, Kingston, Tasmania 7050, Australia

Received 10 March 2011; revised 7 April 2011; accepted 15 April 2011

Available online 23 April 2011

Abstract

A Geographic Information System (GIS)-based investigation into the interannual variability of sea ice concentration was conducted in the Dumont d'Urville Sea off the Terre Adélie coastline, south of 65°S and between 139 and 146°E. Sea ice concentration data derived from Advanced Microwave Scanning Radiometer-EOS (AMSR-E) data were analysed for the period 2003 to 2009. Sea ice concentration was found to be least variable in three regions, namely the Buchanan Bay/Watt Bay region (143–145°E), along ~65.5°S (west of 144.5°E), and the Adélie Bank northeast of Dumont d'Urville near 66°S, 140.5°E. The remaining areas had relatively high interannual variability, in particular the Adélie Basin (~66°S, ~140°E) and the outer fringe of the Mertz Glacier Polynya (MGP). In general, higher sea ice concentration conditions were experienced in the west of the study area (i.e., where annual fast ice recurs), and open water dominated in the MGP and in the northeast. The years 2007–2009 experienced greater persistence of higher sea ice concentration than earlier years. This study provides a baseline for assessing changes in the regional sea ice regime that may occur since the calving of the Mertz Glacier in February 2010.

© 2011 Elsevier B.V. and NIPR. All rights reserved.

Keywords: Sea ice concentration; East Antarctica; Interannual variations; Climatology; GIS

1. Introduction

The term sea ice describes all ice found at sea which has originated from the freezing of seawater (WMO, 1970). There is a distinction between pack ice, which is sea ice that moves in response to forces such as ocean currents and wind, and fast ice, which is sea ice that

* Corresponding author. Spatial Information Science within School of Geography and Environmental Studies, University of Tasmania, Private Bag 76, Hobart, Tasmania 7001, Australia. Tel.: +61 438833261.

E-mail address: mfallows@utas.edu.au (M.B. Smith).

remains largely stationary by forming and remaining mechanically fixed to the shore or grounded icebergs. Sea Ice Concentration (SIC) refers to the percentage of ocean covered by sea ice within a given area, while sea ice extent describes the area of the ocean that is affected by sea ice at any given time (usually demarcated by the 15% ice concentration isoline).

Sea ice covers 4–6% of Earth's ocean surface area and is highly variable on a wide variety of timescales (Gloersen et al., 1992). Antarctic sea ice undergoes a fivefold increase in extent annually from a summer minimum of $3\text{--}4 \times 10^6 \text{ km}^2$ (in February) to a winter maximum of $19 \times 10^6 \text{ km}^2$ (in September–October) (Comiso, 2003). The annual expansion and contraction of sea ice coverage is determined by large-scale, climatological patterns of atmospheric and oceanic circulation and temperature (Gloersen et al., 1992), and is regarded as one of the largest annual geophysical and albedo variations on Earth (Comiso, 2003).

While much attention has recently focussed on trends in Antarctic sea ice extent and seasonality e.g., SCAR (2009) and Stammerjohn et al. (2008) respectively, interannual variability is another key factor that requires better understanding. Spatio-temporal change and/or variability in sea ice coverage are sensitive indicators of climate change and/or variability (IPCC, 2007). Sea ice also plays an important role in the global climate system via its contribution to dense saline water production as a result of sea ice formation (Williams et al., 2008), which in turn is a major driver of global ocean circulation (Rintoul, 1998). Furthermore, Kellogg (1975) predicted an amplification of climate change effects on sea ice through sea ice-albedo feedback (Brandt et al., 2005; Comiso, 2003).

Antarctic marine ecosystems are also strongly linked to the seasonal variability in sea ice advance and retreat (Massom and Stammerjohn, 2010; Smith et al., 2003; Stammerjohn et al., 2008). Sea ice regulates the light regime in the underlying water column (Eicken, 1992) and provides a range of habitats for many plants and animals that have adapted to the conditions (e.g., McMinn et al., 2000; Thomas and Dieckmann, 2010). Ice algae, which can grow under and within sea ice at very low levels of illumination (Loots et al., 2009), form a major energetic link to higher trophic levels, including seabirds and mammals (Arndt and Swadling, 2006; Tynan et al., 2010). Relationships have also been proposed between krill recruitment/abundance and sea ice extent in the Antarctic Peninsula region (Loeb et al., 1997), although the wider applicability of such conceptual models to other regions remains unclear (Massom and Stammerjohn, 2010).

Major changes are occurring in the sea ice covers of both polar regions. While the long-term trend for Arctic sea ice areal extent is negative, the trend in total zonally-averaged extent around the Antarctic continent is on the order of $0.9 \pm 0.2\% \text{ decade}^{-1}$ for the period 1979–2006 (Comiso, 2003). The coincident trend in ice area is slightly more positive at $1.6 \pm 0.2\% \text{ decade}^{-1}$, related to a positive trend in SIC of $\sim 0.93 \pm 0.13\% \text{ decade}^{-1}$ (SCAR, 2009). Substantial regional variability is apparent, however, with decreasing trends in both the extent and seasonality in the West Antarctic Peninsula region (associated with rapid regional warming and changing patterns of oceanic and atmospheric circulation [Massom et al., 2006, 2008; Vaughan et al., 2003]) “counterbalanced” by opposing trends in the Ross Sea sector (Cavalieri and Parkinson, 2008; SCAR, 2009; Stammerjohn et al., 2008; Zwally et al., 2002). Such change has important physical and biological implications, as does variability and extreme events (Massom and Stammerjohn, 2010).

Compared to West Antarctica, relatively little is known about recent change and/or variability in key East Antarctic regions. One such region is the Dumont d'Urville Sea off the Terre Adélie coast, which has been the focus of considerable recent field research and is the focus of this paper. The “icescape” in this region constitutes a number of interlinked large-scale components (Massom et al., 2001), comprising i) a recurrent zone of annual fast ice; ii) an annual cover of pack ice that largely melts back to the coast in summer; and iii) the globally-significant Mertz Glacier Polynya (MGP). A polynya is defined as a recurrent area of anomalously thin and/or low concentration sea ice where, considering the climatological conditions, high sea ice concentration levels would be expected (WMO, 1970; Barber and Massom, 2007).

At its maximum extent, the fast ice in this region extends $\sim 100 \text{ km}$ offshore, and from roughly the Dibble Iceberg Tongue in the west (at $\sim 134^\circ \text{E}$) to Commonwealth Bay in the east (Massom et al., 2009; Fraser et al., Submitted for publication; Fig. 1), where it is closely coupled to the MGP (Barber and Massom, 2007). A key factor in the formation, recurrence and persistence of this feature is the presence of a series of small icebergs grounded on the Adélie and Dibble Banks offshore from Dumont d'Urville, in waters shallower than $\sim 400 \text{ m}$ (Massom et al., 2001; Giles et al., 2008; Fraser et al., Submitted for publication). These icebergs intercept and trap passing pack ice and act as anchor points for fast ice formation (by thermodynamic growth). From initial formation (typically each April), the fast ice grows westwards by the pack ice interception, notably by groups of grounded icebergs in the vicinity of $\sim 66^\circ \text{S}$, 142°E .

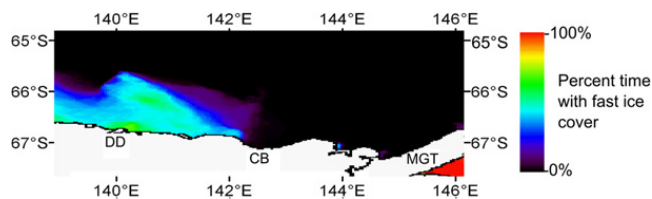


Fig. 1. Fast ice 8.8-year mean for the period March 2000–December 2008 (after Fraser et al., Submitted for publication), derived from 20-day composites of NASA Terra and Aqua Moderate-Resolution Imaging Spectroradiometer (MODIS) visible and thermal infrared satellite imagery (details given in Fraser et al., 2010). DD is Dumont d'Urville; CB Commonwealth Bay; and MGT Mertz Glacier Tongue. The coastline is masked using data from Scambos et al. (2007).

A key factor affecting fast ice formation and persistence offshore from Dumont d'Urville is the Adélie Basin, which runs northwest from the station to the continental shelf break (see Fig. 2). Fast ice is more unstable in this region due to the lack of grounded icebergs in this trough (Fraser et al., Submitted for publication; Massom et al., 2009). Ephemeral fast-ice breakouts (and subsequent re-formations) occur in this region throughout the fast ice season, the timing, frequency and magnitude of which are crucial for the Emperor penguin (*Aptenodytes forsteri*) population at Pointe Géologie during the breeding season (Massom et al., 2009). Fast ice breakout here is largely related to wind strength and direction, but may also seasonally be affected by the presence/absence of a protective pack ice cover (Massom et al., 2009). The fast ice largely melts back to the coast each summer, although substantial interannual variability occurs in the timing (Fraser et al., Submitted for publication; Massom et al., 2009).

The trend in sea ice extent in the Western Pacific Ocean (90–160°E), which includes the Dumont d'Urville Sea, is slightly positive ($+0.7 \pm 0.6\%$ decade⁻¹) (SCAR, 2009). East Antarctic fast ice comprises between 3.8% (during the winter maximum) and 19% (summer minimum) of overall sea ice extent, and by area, between 4.5% (winter) and 30% (summer) (Fraser et al., 2010). The trend in fast-ice extent in the Western Pacific

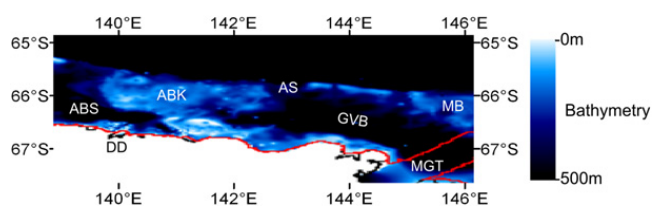


Fig. 2. Bathymetric features of the study area, where ABS is Adélie Basin; ABK Adélie Bank; AS Adélie Sill; GVB George V Basin; MB Mertz Bank; DD Dumont d'Urville; and MGT Mertz Glacier Tongue. Bathymetric data are from Smith and Sandwell, (1997). The coastline is masked using data from Scambos et al. (2007).

Ocean sector from 2000 to 2008 is slightly negative, but not statistically significant ($-0.40 \pm 0.37\%$ year⁻¹) (Fraser et al., Submitted for publication).

An important factor contributing to the formation and maintenance of the MGP is the omnipresence of strong and cold gravitational winds (katabatic winds) which drain seawards from the high ice sheet interior via coastal valleys to generate rapid sea ice formation and drive the ice away from the coastal area as quickly as it forms (Wendler et al., 1997). Together with the Mertz Glacier tongue at $\sim 67^\circ\text{S}$, $\sim 145^\circ\text{E}$ (and an associated northward “finger” of small grounded icebergs [Massom et al., 2001]), which until its calving in February 2010 (Young et al., 2010) extended ~ 80 km into the westward-flowing Antarctic Coastal Current to block the westward advection of sea ice, this creates an extensive area of open water and/or thin ice which recurs each sea ice season and persists for extended periods (Massom et al., 2001). The MGP switches from being a sea ice “factory” in autumn–winter (Barber and Massom, 2007) to a region of enhanced melt (Massom et al., 2003) and enhanced biological production (Arrigo and van Dijken, 2003) in spring–summer. Though the MGP accounts for only $\sim 0.001\%$ of the total area of the Southern Ocean covered by sea ice, it is responsible for $\sim 1\%$ of total annual sea ice production (Tamura et al., 2008). The winter ice growth rate in the MGP (in August 1999) was estimated at ~ 4 cm day⁻¹ by Lytle et al. (2001). The annual average polynya area for the period June–October (1987–1994) was estimated to be 23,000 km² by Massom et al. (1998). An outcome of these characteristics is that the MGP is a major producer of Antarctic Bottom Water, and as such makes a globally-significant contribution to global ocean thermohaline circulation and thus climate (Bindoff et al., 2001; Rintoul, 1998). Another contributing factor is summer upwelling of relatively warm Modified Circumpolar Deep Water (MCDW) onto the shelf via the Adélie Sill. This not only enhances melting of sea ice but also provides additional high salinity water to the shelf (Rintoul, 1998). The MCDW mixes with the High Salinity Shelf Water (HSSW) that is formed by brine rejection within the MGP during sea ice formation to form Adélie Land Bottom Water (ALBW) (Rintoul, 1998).

Prior to its calving, the Mertz Glacier tongue was the largest in the area, with several other smaller glaciers occurring along the coast to the west, including the Astrolabe Glacier at $\sim 140^\circ\text{E}$. Rifting of the Mertz Glacier tongue was monitored via GPS beacons located on the glacier from 2007 (Legrésy et al., 2010) with the expectation that a major calving event would occur. The calving created a major iceberg of dimensions $\sim 40 \times \sim 80$ km, designated C28 (Young et al., 2010), which broke into

smaller sections in April 2010. These sections drifted across the edge of the continental shelf by the end of that month. Another major change to the regional “icescape” has been the realignment and movement in the MGP domain of vast iceberg B9B (Young et al., 2010), which was originally grounded to the east of the Mertz Glacier (Massom, 2003) before ungrounding in early 2010 to possibly play a key role in the abrupt calving of the glacier tongue. These abrupt and dramatic changes are expected to have an effect on the size and productivity of the MGP, with implications for the sea ice regime, marine ecosystems and global currents (Kusahara et al., 2011).

The aim of this paper is to analyse SIC in the Dumont d’Urville Sea near Terre Adélie in order to identify mesoscale regions where the annual sea ice regime has remained similar throughout the study period 2003–2009, and to identify areas of lowest and greatest variability. An overarching aim is to provide key physical information i.e., on annual sea ice coverage characteristics and their variability, compatible with annually sampled *in situ* species distribution data, against which to evaluate findings within the Collaborative East Antarctic Marine Census (CEAMARC) (www.caml.aq) and Integrated Coastal Oceanography Observations in Terre Adélie (ICO²TA) (www.koubbi@obs-vlfr.fr) programmes. These linked programmes are working to develop an ecoregionalisation framework and gauge and understand the impact of climate (environmental) change on regional biodiversity and ecosystem structure and function. Detailed analysis of the cause of observed sea ice variability, related to atmospheric and oceanic forcing, is beyond the scope of this paper.

The study area of both the CEAMARC and ICO²TA projects is located on the George V Shelf, which has an average depth of ~500 m at the shelf break (Beaman et al., 2010). The main bathymetric features of the shelf, illustrated in Fig. 2, are the George V Basin, which reaches depths of 1300 m adjacent to the Mertz Glacier, and the Adélie Sill (~66°S, 143°E). The Adélie Bank and Mertz Bank are located to the west and east (respectively) of the George V Basin, and have an average depth of 200 to 250 m (Beaman et al., 2010). The Adélie Basin extends from near the coast south of the Adélie Bank (northwest of Dumont d’Urville, (66.5°S, 140°E)) where it reaches depths of ~1000 m, to the shelf edge.

2. Datasets and methods

2.1. Sea ice concentration (SIC) data set

Variability in SIC was investigated within the area 65°–67.5°S, 139°–146°E using daily AMSR-E

(Advanced Microwave Scanning Radiometer-EOS) ARTIST Sea Ice (ASI) algorithm data with a spatial resolution of 6.25 km (Spren et al., 2008). These data were obtained for the period 2003 to 2009 from the Centre for Marine and Atmospheric Sciences (ZMAW) at Hamburg University. Details of the AMSR-E instrument, which has been operating since May 2002, are given in Heinrichs et al. (2006). The ASI algorithm uses an empirical model to retrieve ice concentration values between 0% and 100% (Spren et al., 2008), with lower frequency channels being used to filter weather effects and to remove spurious SIC values in open water areas. In the Geotiff file format available from ZMAW, SIC values of 0%–100% are scaled to cell values 0 to 200. A subsample of one Geotiff from each week was used in the analysis. Future work may, however, benefit from daily analyses, given that sea ice conditions can change dynamically within a week.

The 6.25 km AMSR-E SIC dataset used in this study represents the highest-resolution daily passive microwave SIC data currently available; however, there are some issues associated with their use for SIC retrieval. Microwave signatures from glacial ice may contaminate coastal cells (Spren et al., 2008). This problem is negated, to some extent, by our removal of cells adjacent to the coast during processing. Low SIC values may have higher associated uncertainties due to the efficacy of the ASI algorithm, and cell values along the ice edge may be too high due to unfiltered weather effects (Spren et al., 2008). These issues may affect retrieval of the size of relatively ice-free features such as the MGP, and may reduce the accuracy of identification of narrow coastal polynyas such as that identified in Commonwealth Bay by Wendler et al. (1997). Fraser et al. (2010) also found that the ASI algorithm sometimes underestimates the concentration of fast ice (as low as ~55% SIC for fast ice regions).

2.2. GIS spatial analysis of sea ice concentration

Mapping and map-based analysis was done using ESRI ArcGIS ArcView 9.3. ArcView Modelbuilder was used to enable custom design of sequences of geoprocessing tools for easy automation and repetition of workflows. The Spatial Analyst/Single Output Map Algebra tool applies custom algebra expressions to all or selected cells within the data sets. The Spatial Analyst/Cell Statistics tool calculates statistics based upon the values of cells in the same location in many layers. The processing completed quickly on a variety of computer hardware.

In this study, our SIC analysis is based on the classification system of the Nautical Institute (Buysse, 2007), whereby SIC is expressed in tenths, and is adapted from

an original suite of seven classes (Table 1; Buysse, 2007) to five classes (Table 2) for ease of interpretation. Each weekly AMSR-E map was geoprocessed in ArcView with each of five algebraic expressions corresponding to the five SIC classes (see Table 2). This produced 52 binary maps per class per year. By annually compositing the binary maps for each class, we produced five annual class maps per year, each of which estimates the number of weeks each class persisted within each 6.25×6.25 km cell. The number of weeks in the annual maps for classes 2, 3, and 4 were generally very low and showed very little variation between cells and between years. Therefore, for the purpose of improved visualization of spatial and temporal variability of SIC, we decided to reduce the five SIC classes to three SIC categories (SICCs) by compositing the annual maps in classes 2, 3 and 4. The three SICCs are as follows: 1) SICC1, 0–10% SIC or ice-free to open water (hitherto abbreviated to the term open water); 2) Transition, 11–79% SIC encompassing a broad range of sea ice conditions from very open ice to close ice; and 3) SICC5, 80–100% SIC or high concentration pack ice/fast ice. A seven-year average map was produced from each of the three sets of annual SICC maps for the purpose of visualising SIC distribution tendencies. Standard deviations for each of the three sets of annual SICC maps were also produced; cell values represent the standard deviation, in number of weeks each year, of SICC experienced during the seven-year study period. The three SICC standard deviation maps were then added together to determine regions of overall low/high interannual variability of SIC.

2.3. Numerical analysis

A Multiple Correspondence Analysis (MCA) (Legendre and Legendre, 1998; Greenacre, 2006) was applied to annual SICC, latitude, longitude, and year data for the purpose of finding evidence of dependence

Table 1

Sea ice concentration for navigational purposes is expressed by the Nautical Institute in tenths, describing the amount of the sea surface covered by ice, as a fraction of the whole area being considered (Buysse, 2007). These categories have been simplified and adapted for the purpose of this study as described in Table 2.

Ratio	Nautical Institute nomenclature
0	Ice-free
<1/10	Open water
1/10 to 3/10	Very open ice
4/10 to 6/10	Open ice
7/10 to 8/10	Close ice
9/10 to <10/10	Very close ice
10/10	Consolidated ice/compact ice

between these data. The MCA method is an extension of Correspondence Analysis (CA) allowing analysis of relationships between multiple categorical dependent variables. The MCA builds an indicator matrix (i.e. a matrix whose entries are 0 or 1) to which a standard CA is applied (Abdi and Valentin, 2007). We used the annual number of weeks of SICC1 and of SICC5 within each grid cell as active information (data of most interest). The Transition category was initially included in the MCA but was found not to affect the results and was subsequently removed. To categorise the active information, the complete set of values for all seven years of the study period in all study area grids was divided into four equal strength modalities (as much as ties in the data would allow, considering that tied values must all be contained within the same modality). For latitude and longitude, we used modalities of 0.5 degrees of arc and 1.0 degrees of arc respectively. Interpretation of the results is based on the proximities between points in the topology.

3. Results

3.1. SICC seven-year averages

The SICC1 seven-year average map (Fig. 3a) shows that a large number of weeks (>17 weeks) of SICC1 (i.e. open water) occurred in: i) the MGP region; ii) across the north of the study region at $\sim 65^\circ\text{S}$; and iii) in a small region centred on 65.75°S , 139.5°E . The latter corresponds to the unstable fast ice region (hitherto referred to as the “Adélie Basin” region), where breakouts occur as a result of lack of fast ice anchor points in the form of grounded icebergs over the Adélie Basin (Massom et al., 2009). The regions with a relatively lower number of weeks of SICC1 (<13 weeks) were: i) an oval region in the west centred on 66°S , 140.5°E which is covered by fast ice for a significant portion of the year; and ii) a tail-like region extending west from 146°E to $\sim 143^\circ\text{E}$ between 65.5°S and 66°S . This “tail” region corresponds to a feature described as the “tongue” by Massom et al. (2001) and Barber and Massom (2007), namely a compact “stream” of thick floes of pack ice drifting westwards along the continental shelf break from east of the MGT/grounded icebergs/fast ice blocking feature.

The spatial distribution in the Transition seven-year average map (Fig. 3b) clearly shows that the MGP experienced in excess of 18 weeks of Transition annually, well above the seven-year Transition median of 7 weeks across the entire study region (see Fig. 4). Values decreased from here in a northwest direction, with many cells west of 142°E experiencing less than four weeks of Transition e.g., regions centred on

Table 2

Sea ice concentration classes for our analysis were based on the Nautical Institute system of sea ice classification (see Table 1). Corresponding AMSR-E raster cell values are in column 3, and the algebraic expressions for geoprocessing in the GIS in column 4. Column 5 lists the corresponding names for the three sea ice concentration categories (SICCs) used in our study.

Class	SIC	AMSR-E value	Algebraic expression	SICC
1	0–10%	0–19	[input] < 20	SICC1
2	11–39%	20–79	[input] > 19 AND [input] < 80	
3	40–59%	80–119	[input] > 79 AND [input] < 120	Transition
4	60–79%	120–159	[input] > 119 AND [input] < 160	
5	80–100%	160–200	[input] > 159 AND [input] < 201	SICC5

66.2°S, 141°E (corresponding with the fast ice zone shown in Fig. 1) and between 65 and 65.5°S, 139–142°E. Two regions form exceptions to this i.e., at least nine weeks of Transition was experienced, namely i) the “Adélie Basin” region, and ii) a region at ~66°S, ~142.5°E (hitherto referred to as the “grounded iceberg” region), located to the west of icebergs grounded on the Adélie Bank.

The SICC5 seven-year average map (Fig. 3c) shows that the MGP region experienced less than 10 weeks of SICC5 per year, as expected for this latent-heat polynya. Cell values increase in a westerly direction, with values greater than 32 weeks dominating the western half of the study area, which is seasonally covered in fast ice (Fig. 1; Fraser et al., 2010). The “Adélie Basin” and “grounded iceberg” regions in the west have low SICC5 values (10–19 weeks). For the “Adélie Basin” region, this reflects the instability of seasonal fast ice here due to the

lack of grounding points for icebergs in deep bathymetry (> ~500 m) (Fraser et al., Submitted for publication; Massom et al., 2009).

The box graph in Fig. 4 represents the cell values from the seven-year average maps of SICC1, Transition, and SICC5 (Fig. 3). The seven-year median for SICC1 was 15 weeks annually, and the Interquartile Range (IQR) was the smallest of the three SICCs, indicating that SICC1 was the least variable SICC. Most cells experienced 7–23 weeks of SICC1 annually, with outliers experiencing values on both sides of this range. The Transition category median was the smallest of the three categories (7 weeks annually). The IQR shows that Transition was slightly more variable annually than SICC1; most regions experienced 0–22 weeks of Transition annually, with outliers experiencing more than 22 weeks annually. SICC5 had the highest median (30 weeks) and largest IQR. Most regions experienced

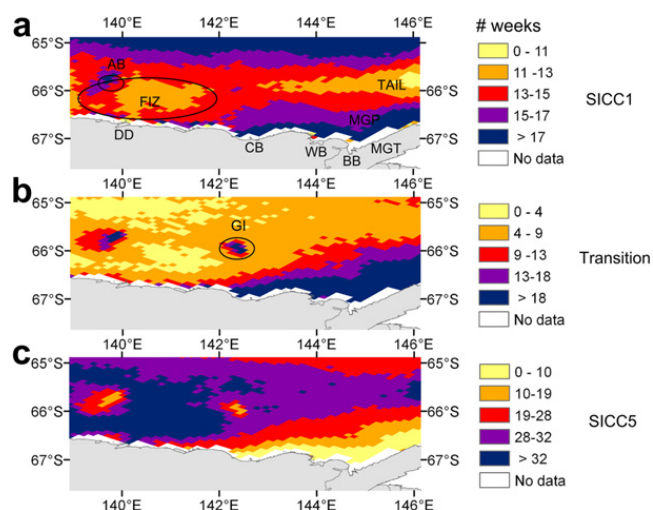


Fig. 3. Seven-year SIC category (SICC) averages for the period 2003–2009, derived from AMSR-E sea ice concentration data. Note that the legend for each SICC is based upon the seven-year mean cell value for that SICC. DD is Dumont d’Urville; CB Commonwealth Bay; WB Watt Bay; BB Buchanan Bay; MGP Mertz Glacier polynya; MGT Mertz Glacier Tongue; AB “Adélie Basin” region; GI “grounded iceberg” region; and FIZ fast ice zone.

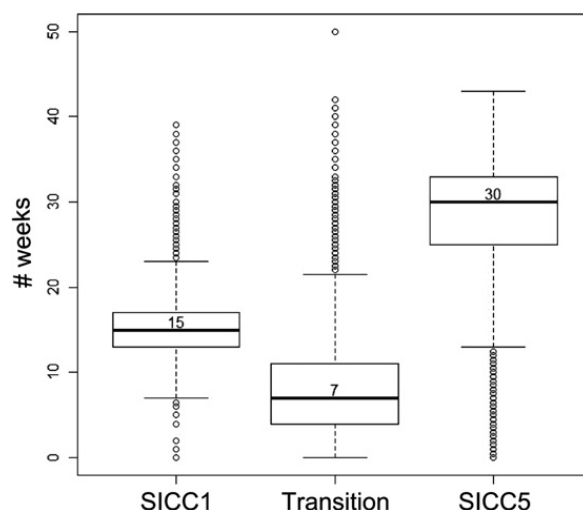


Fig. 4. Box-plots of 7-year average annual number of weeks that each 6.25 km-resolution raster cell experiences each SIC category. The lower and upper bounds of the box represent the first and third quartiles, respectively, or the interquartile range (IQR). The horizontal line inside the box indicates the location of the median. Vertical dashed lines terminate at 1.5 IQR. Individual points represent extreme values.

12–42 weeks of SICC5 annually, although outliers experienced SICC5 for less than 12 weeks annually.

3.2. Interannual spatial variability of sea ice concentration

Fig. 5 shows the yearly number of weeks in each SICC. Many weeks of SICC1 (>17 weeks annually) consistently occur in a narrow strip on the coast east of 142.5°E and along the western edge of the Mertz Glacier (i.e., in the MGP and along the coast to

Commonwealth Bay). In the years 2004–2006, the strip is longer (although not continuous) and extends eastwards as far as 139°E to capture the polynya identified in Commonwealth Bay by Wendler et al. (1997). To the north of the study area, at 65°S, to ~65.5°S, is a feature of high number of weeks of annual SICC1. However, this feature is barely visible in 2003 and 2008, and in 2005 it is only visible to the east of ~141°E. This feature is particularly latitudinally extensive in 2004 and 2006, with open water occurring here for longer during these two years.

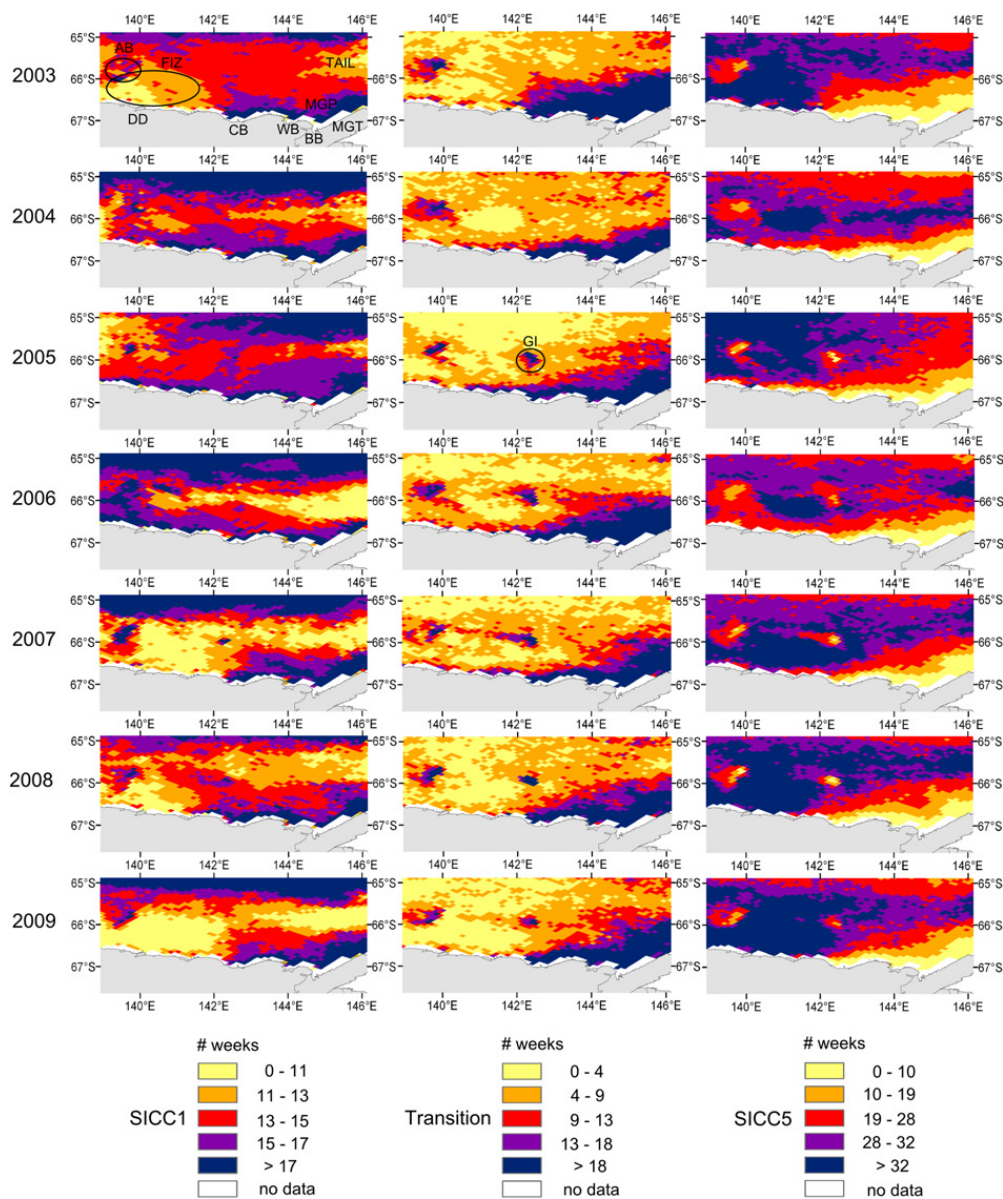


Fig. 5. Interannual spatial variability of number of weeks of SIC in three categories. Each annual SICC map shows the number of weeks during which each raster cell experiences one SIC category. The legends are based on seven-year mean cell values (see Fig. 3). DD is Dumont d’Urville; CB Commonwealth Bay; WB Watt Bay; BB Buchanan Bay; MGP Mertz Glacier polynya; MGT Mertz Glacier Tongue; AB “Adélie Basin” region; GI “grounded iceberg” region; and FIZ fast ice zone.

Maps of all years (Fig. 5) show the “tail” region as low value SICC1 cells (<13 weeks annually) of varying sizes that extend westwards along $\sim 65.5\text{--}66^\circ\text{S}$, from 146°E , corresponding with the “tongue” (Massom et al., 2001; Barber and Massom, 2007). The “tail” is smallest in 2003, 2004, and 2005, and is largest in 2006–2009. Another patch of low values of SICC1 (≤ 11 weeks annually) occurs in the western half of the study area in all years, the location and size of which varies annually (this appears to be related to the interannual variability in the fast ice zone). In 2003 and 2008 this patch occurs from the coast at 139°E to $\sim 141^\circ\text{E}$ and extends north to 66°S . In 2004, the patch is just visible on the western edge of the study area south of 66°S . In 2005, it is located north of 66°S at the western edge of the study area, and in 2006 it is not visible at all. The largest patch occurs in 2007 and 2009, extending from the coast between ~ 140 to $\sim 142^\circ\text{E}$ (in 2007), and 139 to $\sim 142^\circ\text{E}$ (in 2009), northward to 65.5°S .

In 2003, the central region of the study area experienced a relatively small range in number of weeks of SICC1 (13–15 weeks). The “Adélie Basin” region is distinguishable in the SICC1 maps of all years as an area of >17 weeks of SICC1, annually centred on $\sim 66^\circ\text{S}$, $\sim 140^\circ\text{E}$. The “grounded iceberg” region at 66°S , 142.5°E is barely distinguishable in SICC1 maps as a region of just a few cells with higher values than those surrounding it (except in 2009 when it is not distinguishable at all). This feature is visible in maps of Transition, as well as SICC1.

Maps of Transition for all years show that a large number of weeks of Transition (>18 weeks annually) were experienced in the MGP region, and further west along the coast in many years (2004, 2005 and 2007). The latitudinal extent of this phenomenon was greatest in 2003. In all years, the western half of the study area predominantly experienced very few weeks of Transition (<4 weeks annually), especially in 2005 (in the north), 2008 and 2009. The “Adélie Basin” and “grounded iceberg” regions are both visible in all years (except 2003 and 2004 when the “grounded iceberg” region is not visible) as small regions of high values (>18 weeks annually) of Transition.

The MGP is visible as a region of low values (<19 weeks annually) in SICC5 maps for all years. The latitudinal extent of this feature was largest in 2003 and smallest in 2004, and extended westward to 139°E during the years 2004–2006. In all years except 2005, the “tail” in the west of the study region, at $\sim 66.5^\circ\text{S}$, is visible as an area of high number of weeks of SICC5, and extends to connect with the fast ice zone (except in 2006 when the “tail” ends at $\sim 144.5^\circ\text{E}$ and

does not connect with the fast ice zone). The amount of pack ice drifting into the study area from east of the MGT varies annually; the reason for this is outside the scope of this study but is likely due to variability in large-scale atmospheric circulation patterns (Massom et al., 2003). The “grounded iceberg” feature was not visible in 2003 and 2004, and is only distinguishable in the annual SICC maps after 2005. SIC was generally higher in the “grounded iceberg” region during 2003 and 2004 than other years.

In the western half of the study area, the “Adélie Basin” and “grounded iceberg” regions are distinguishable as small regions of low value SICC5 cells (<4 weeks annually), except in 2003 and 2004 when the “grounded iceberg” region is not distinguishable. Cells with much higher values (≥ 28 weeks annually) surround these features. A region of interannually-variable size, which typically experiences more than 37 weeks of SICC5, is situated between the “Adélie Basin” and “grounded iceberg” regions. This feature is interpreted to be seasonally-recurring fast ice of interannually varying extent; it reached a maximum extent in 2009, while the smallest features occurred in 2004 and 2006. In 2005, a high number of weeks of SICC5 (>32 weeks) occurred throughout the north-western sector of the study region. This is interpreted as being compact pack ice, since the Fraser et al., (Submitted for publication) fast ice dataset does not show particularly extensive fast ice during that year.

The box diagrams in Fig. 6 represent the cell values for each annual SICC map. For SICC1, the four years with the lowest medians (2003, 2007–2009) are the same years that have the highest medians in SICC5. The year 2003 stands out from other years because the IQR for SICC1 is very small (8 weeks). These points are relevant to the MCA where a relationship between the number of weeks of SICC1 and SICC5 is illustrated (see below), and the years of the study period are grouped according to the location and annual duration of these two SICCs.

3.3. Multiple Correspondence Analysis (MCA)

Fig. 7 shows the output of the MCA, which reduced the multi-dimensional dataset into a two-dimensional map, or topology, producing a summary of SIC inter-annual variability in one graph. This plan represents 44.6% of the total information with 25.35% for the first axis and 19.26% for the second axis. The topology is characterized by the U-shaped curves of the SICC1 and SICC5 modality limits increasing in opposite directions. The continuous, and generally opposite, trends

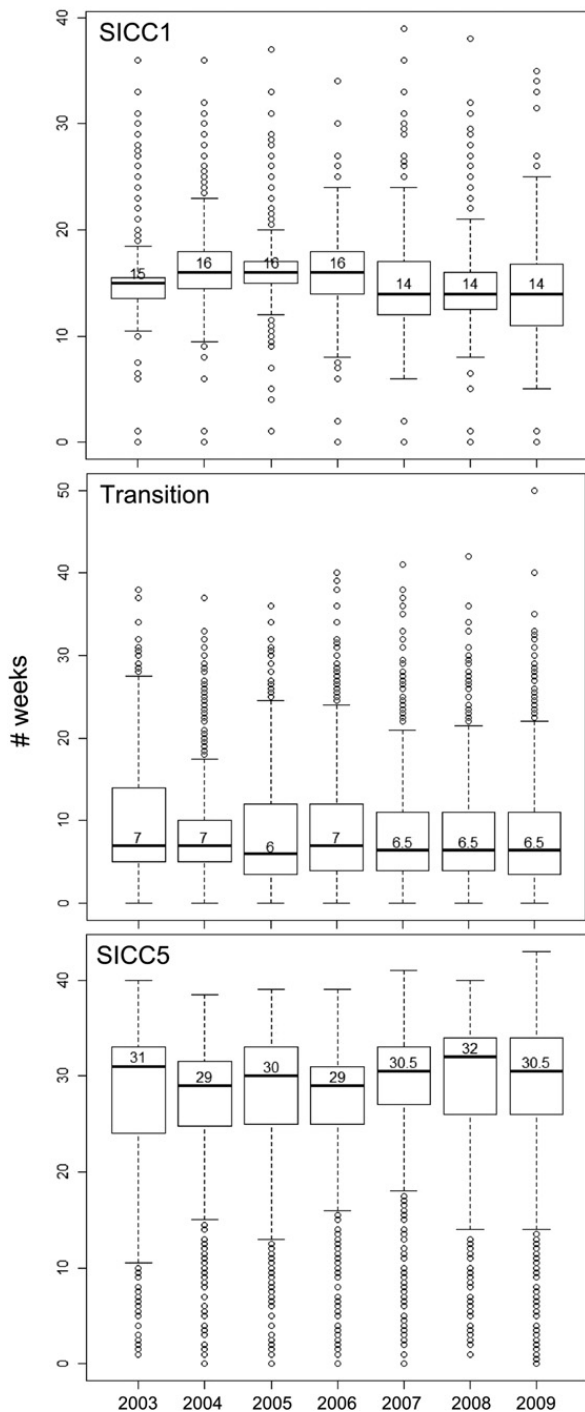


Fig. 6. Box plots of annual SIC data in three categories (see Fig. 4 for description).

between SICC1 and SICC5 reflect an opposite dependence between these two variables i.e., on one hand, regions with high number of weeks of SICC1 and low number of weeks of SICC5, and, on the other hand, regions with the opposite pattern. These trends were expected given that, with the exception of the MGP region, the annual Transition phase between sea ice extremes is generally relatively brief throughout the

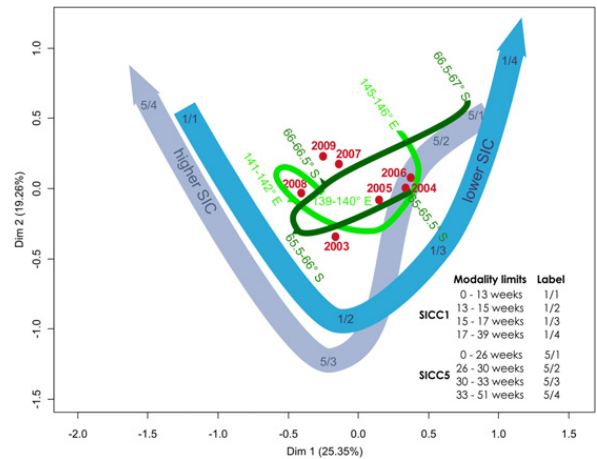


Fig. 7. MCA results derived using SICC1 and SICC5 as active information, and the year, latitude and longitude as illustrative information. The modality limits for the active parameters, and their corresponding labels, are listed. For enhanced interpretation a line in order of value from smallest to largest connects the positions of the modalities of SICC1, SICC5, latitude and longitude. Some latitude and longitude modality labels have been omitted to draw attention to regions discussed in Section 3.3.

study area. The positions of the years on the topology give supplementary information about the interannual variability of SICC1 and SICC5. The relatively close proximity of the years 2007, 2009, and to a lesser extent, 2008, coupled with their positions in relation to other years and to the U-shaped curves of SICC1 and SICC5 suggests evidence of a relatively (for the study period) high number of weeks of SICC5 associated with a relatively low number of weeks of SICC1. The inverse “global” characteristic is shown by the positions for the years 2004, 2005 and 2006, suggesting that sea ice concentration was lower. The year 2003 has a more intermediate position.

The positions of latitude and longitude on the topology give supplementary information about the seven-year spatial tendencies of SICC1 and SICC5. The shape and direction of the longitudinal curve suggests that sea ice concentration was generally higher in the west than in east of the study region. The latitudinal curve adheres less to the U-shaped pattern described by SICC1, SICC5 and longitude, and suggests that sea ice concentration was generally higher through the middle of the study region than in the north and south. Evidence of regional tendencies of sea ice concentration can be gained by observing the location on the topology of both latitudinal and longitudinal modalities together. The region within 65.5–66.5°S and 139–142°E is characterized by high sea ice concentration (i.e. it is the fast ice zone). Two regions, within 65–65.5°S and 142–146°E and 66.5–67°S and 142–146°E, are

marked by low sea ice concentration (north of the study region, and the MGP, respectively). These regional tendencies can also be seen in the seven-year maps of SICC1 and SICC5 (Fig. 3).

3.4. Sea ice concentration standard deviation maps

Standard deviation maps (see Fig. 8) show that SICC1 displays the least interannual variability of all the categories i.e., $1\sigma \leq 3$ weeks for the entire study area, except for the coastal region west of 142°E and a few cells with larger standard deviations. The Transition variability map (Fig. 8b) shows that most regions experience relatively low interannual variability in Transition conditions ($1\sigma \leq 3$ weeks). However, Transition conditions in the “Adélie Basin” and “grounded iceberg” regions, and the offshore edge of the MGP, are more variable. SICC5 is the most variable category i.e., few cells with $1\sigma \leq 2$ weeks, and many with $1\sigma \leq 4$ weeks. The “Adélie Basin” and “grounded iceberg” regions, the offshore edge of the MGP and the coastal region from 139 to 142°E are more variable in SICC5 than other regions.

Variability of SIC conditions in general is represented by Fig. 8d, which is derived from the sum of standard deviations ($\Sigma\sigma$) in SICC1, Transition, and SICC5 (Fig. 8a–c). Fig. 8d shows that SIC is least variable ($\Sigma\sigma \leq 6$ weeks) in three regions i.e., the MGP region, along ~ 65 – 65.5°S , west of 144.5°E (dipping south to 66°S between 142.5 and 144°E), and a small patch centred on $\sim 66^\circ\text{S}$, $\sim 140.5^\circ\text{E}$. The latter coincides with annual fast ice that occurs over the Adélie Bank (Fraser et al., 2010; Massom et al., 2009), where the average water depth is 200–250 m (Post et al., 2010). The remaining areas were more variable from year to year. In particular, we note high interannual variability ($\Sigma\sigma > 9$ weeks) in a triangular region extending from the “Adélie Basin” region to the coast at 139 – 142°E , reflecting the interannual variability of fast ice in the region to the west of Dumont d’Urville and above the Adélie Basin. As the bathymetry here is too deep for the grounding of icebergs (Beaman et al., 2010), fast ice in this region tends to be relatively unstable (Massom et al., 2009). Another region of high interannual SIC variability is the “grounded iceberg” region.

The region along the line of ~ 66 – 66.5°S , east of 142°E and corresponding with the offshore edge of the MGP, also appears in Fig. 8d as a region of high interannual variability. This may be an indication of variability in the size of the MGP due to wind variability (Tamura et al., 2007), and the relationship between the development (and timing) of the “tongue” and the size of the MGP; the increased blocking ability

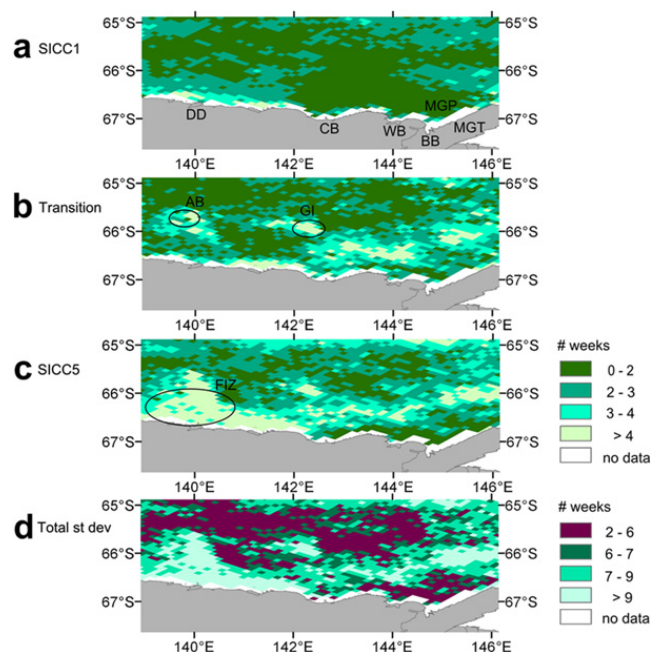


Fig. 8. Variability in SIC is derived from the total standard deviation between years of each of the three SIC categories: a) SICC1, b) Transition, and c) SICC5. d) A map of variability of SIC conditions during the period 2003–2009, derived from the sum of a), b) and c). DD Dumont d’Urville; CB Commonwealth Bay; WB Watt Bay; BB Buchanan Bay; MGP Mertz Glacier polynya; MGT Mertz Glacier Tongue; AB “Adélie Basin” region; GI “grounded iceberg” region; and FIZ fast ice zone.

of a well-developed “tongue” leads to more open ice conditions around a smaller polynya opening (Massom et al., 2001).

4. Discussion and conclusions

Given the caveats outlined in Section 2.1, our study has produced a summary of interannual variability of SIC in the Adélie Land region, in a form that is compatible with *in situ*-sampled species distribution and physical parameter data acquired over the period 2003–2009. In effect, our annual average SICC map data can be used as a “baseline” parameter for ecoregionalisation and can therefore contribute to gauging and understanding the effects of climate variability on Antarctic marine ecosystems. The analysis also enables identification of regions where the combination of number of weeks of open water and sea ice (and a broad category of states in between) is similar each year. In the process, our study has also identified the interannual variability in the size and location of known sea ice features such as the MGP, the zone of annual fast ice offshore from Dumont d’Urville, and the “Adélie Basin” and “grounded iceberg” regions. Our study has shown that SIC in the study area, with the exceptions of the MGP, the “Adélie Basin” and

“grounded iceberg” regions, is generally either extremely low (SICC1) or extremely high (SICC5) and that the duration of transition between the two extremes is generally relatively brief.

A statistical analysis of trends in sea ice concentration is beyond the scope of this research, given the short period analysed. Nevertheless, we observe in the MCA (Fig. 7) that the years 2007–2009 experienced more weeks of high SIC and fewer weeks of low SIC than other years. These findings broadly agree with the positive sea ice extent/area trends in the Western Pacific Ocean sector reported in other research (e.g., Cavalieri and Parkinson, 2008; Comiso, 2003; Zwally et al., 2002). However, our study is unique in that it investigates persistence of Antarctic SIC for the first time (Fig. 8).

Most of the fast ice zone was found to display considerable interannual variability, particularly above the Adélie Basin; this is consistent with the findings of Massom et al. (2009). Interannual variability in SICC5 of >19 weeks was considerable in this region (see Fig. 5). However, the seven-year average values of >32 weeks of SICC5 across the fast ice zone (see Fig. 3) exceed the findings of Fraser et al. (submitted for publication), who found that fast ice occurred near Dumont D'Urville Station for ~40% of the year on average between 2000 and 2008. It must be noted here that AMSR-E measurements cannot inherently distinguish between moving and fast ice, which explains, to some extent, the discrepancy between the fast ice average of Fraser et al. (2010) and the seven-year SICC5 average in our study. In their study of fast ice distribution and variability in the Western Pacific Ocean sector of Antarctica (90–160°E) for the years 2000–2008, Fraser et al., (Submitted for publication) found a slight, but non-significant decrease in fast ice extent. Our study indicates that sea ice concentration conditions in the Terre Adélie region do not reflect fast ice conditions in the broader Western Pacific Ocean sector.

As revealed in the MCA topology (Fig. 7) and in the seven-year average maps of SICC1 and SICC5 (Fig. 3a and c), these two SIC categories appear to be anti-correlated. Another anti-correlation is observed in Fig. 3 that was not detectable in the MCA - in regions where the number of weeks of Transition is high, the number of weeks of SICC5 is low, particularly in the MGP, “Adélie Basin” and “grounded iceberg” regions. This highlights the significance of the Transition category, which encompasses a large range of SIC values (11–79% SIC). Our analysis of SIC may be improved by increasing the number of SIC categories to four. In that case, we would be able to make better

assumptions about SIC in the MGP, the “Adélie Basin” and “grounded iceberg” regions, areas that experience many weeks of Transition annually.

Another relationship between Transition and SICC5 can be seen in the annual SICC maps (Fig. 5). The inverse of the relationship discussed above is apparent i.e., areas of many weeks of SICC5 that experience very few weeks of Transition. This relationship is most evident (in all years) in areas of the fast ice zone between the “Adélie Basin” and “grounded iceberg” regions, and also in 2005 in the northwest region of the study area. These regions can be interpreted as areas of abrupt change, where open water conditions convert very quickly to heavy sea ice conditions, to effectively bypass the Transition stage. Heavy sea ice conditions predominate for many months, reverting very quickly to open water conditions in the summer melt season.

The MCA topology identifies an area of high number of weeks of SICC1 within 66.5–67°S, 142°–146°E coinciding with the location of the MGP. However, no such distinction is apparent in the MCA for the “Adélie Basin” or “grounded iceberg” regions. This is because the latitude and longitude modalities used in the MCA are too broad (0.5 and 1.0 degree of arc respectively) to capture the spatial characteristics of these small features.

In previous studies, SIC variability in Antarctica has been largely analysed through monthly sea ice extent/area anomalies (e.g., Cavalieri and Parkinson, 2008) and 20-day composites of East Antarctic fast ice extent (Fraser et al., Submitted for publication). Considerable work is also being carried out on regional changes and variability in sea ice seasonality e.g. Stammerjohn et al. (2008), and their potential impact on phenological relationships (Arrigo et al., 2002; Ducklow et al., 2007; Massom and Stammerjohn, 2010). In conclusion, our study adds an additional layer in the form of analysis of the seasonal variability of sea ice concentration in a key East Antarctic region. While a seven-year period is not sufficient to make assumptions about long-term trends in spatio-temporal patterns of sea ice concentration, it can provide a baseline with which to compare future changes in the sea ice regime. It is planned to extend back in time (to 1979), albeit at a lower spatial resolution of 25 km, using data from previous-generation passive microwave sensors i.e. Scanning Multichannel Microwave Radiometer (1979–1987) and Special Sensor Microwave/Imager (1987–present).

While 6.25 km-resolution AMSR-E data are suitable for investigating the overall sea ice conditions in the region, ecoregionalisation necessitates distinction

between ice type, age and thickness, because different species and their life-stages are associated with different sea ice conditions (Thomas and Dieckmann, 2010). This will require incorporation of data from a range of additional satellite sensors, including CryoSat-2.

Future work needs to also incorporate information on causes of observed annual variation in the spatial distribution and concentration of sea ice within the Dumont d'Urville Sea i.e., local and remote weather conditions and ice features (including extreme events e.g., Massom et al., 2006), and fixed variables such as coastal and bathymetric features. Furthermore, the dynamics of sea ice conditions within a region must be contextualised by observing sea ice conditions in neighbouring regions. In this case, the “upstream” area (east of the Mertz Glacier) is particularly influential to the MGP and therefore the Terre Adélie region (Barber and Massom, 2007; Massom et al., 2001).

Subsequent analyses should also take into account abrupt events. Such as the large calving of the MGT in February 2010 (Young et al., 2010). Despite the resultant shortening of the remaining tongue to ~20 km, the MGP largely appears to have returned to its sea ice “factory” role. However a decrease in the production of dense shelf water, with implications for climate, is expected to occur since the “icescape” of the area has been significantly altered (Kusahara et al., 2011; Young et al., 2010). Major changes in the length of the Mertz Glacier and the associated realignment and movement of vast iceberg B9B are expected to have an effect on the regional sea ice regime, and plans are in place to detect and analyse the effects by applying our method to more recent and future data.

Acknowledgements

For MS, this research was part of an exchange between the University of Tasmania (UTAS) and Université Pierre et Marie Curie organised through the International Antarctic Institute. AMSR-E ASI sea-ice concentration data were obtained from the University of Hamburg (<ftp://ftp-projects.zmaw.de/seaiice/>). IMAS, and Spatial Information Science within the School of Geography and Environmental Studies at UTAS provided funding. Thanks also to Robert Anders and James Culverhouse at UTAS for providing the ArcView licence. Many thanks to Patti Virtue (IASOS) for logistical support, and Stanislas Zamora (captain of RV *l'Astrolabe* for 2009–2010 ICO²TA expedition) for Nautical Institute sea ice classification information. For AF and RM, this work was supported by the Australian Government's Cooperative Research Centre

program through the ACE CRC, and for RM contributes to AAS Project 3024. This work is related to the ICO²TA programme of IPEV (PI. Philippe Koubbi), the Zone Atelier Antarctique of CNRS (PI. Marc Lebouvier) and ANR Glides (PI. Charles-André Bost).

References

- Abdi, H., Valentin, D., 2007. Multiple correspondence analysis. In: Salkind, N. (Ed.), *Encyclopedia of Measurement and Statistics*. Sage, California, pp. 1–13.
- Arndt, C.E., Swadling, K.M., 2006. Crustacea in Arctic and Antarctic sea ice: distribution, diet and life history strategies. *Adv. Mar. Biol.* 51, 197–315.
- Arrigo, K.R., van Dijken, G.L., 2003. Phytoplankton dynamics within 37 Antarctic coastal polynyas. *J. Geophys. Res.* 108 (C8), 3271 doi:10.1029/2002JC001739.
- Arrigo, K.R., van Dijken, G.L., Ainley, D.G., Fahnestock, M.A., Markus, T., 2002. Ecological impact of a large Antarctic iceberg. *Geophys. Res. Lett.* 29 (7), 1104, doi:10.1029/2001GL014160.
- Barber, D.G., Massom, R.A., 2007. The role of sea ice in Arctic and Antarctic polynyas. In: Smith, W.O., Barber, D.G. (Eds.), *Polynyas: Windows to the World's Oceans*. Elsevier, Amsterdam, pp. 1–54.
- Beaman, R.J., O'Brien, P.E., Post, A.L., de Santis, L., 2010. A new high-resolution bathymetry model for the Terre Adélie and George V continental margin, East Antarctica. *Antarct. Sci.* 22, 371–378.
- Bindoff, N.L., Williams, G.D., Allison, I., 2001. Sea-ice growth and water-mass modification in the Mertz Glacier polynya, East Antarctica, during winter. *Ann. Glaciol.* 33, 399–406.
- Brandt, R.E., Warren, S.G., Worby, A.P., Grenfell, T.C., 2005. Surface albedo of the Antarctic sea ice zone. *J. Clim.* 18, 3606–3622.
- Buysse, J., 2007. *Handling Ships in Ice*. The Nautical Institute, London.
- Cavaleri, D.J., Parkinson, C.L., 2008. Antarctic sea ice variability and trends, 1979–2006. *J. Geophys. Res.* 113, C07004 doi:10.1029/2007/JC004564.
- Comiso, J.C., 2003. Large scale characteristics and variability of the global sea ice cover. In: Thomas, D.N., Dieckmann, G.S. (Eds.), *Sea Ice: An Introduction to Its Physics, Biology, Chemistry, and Geology*. Blackwell Publishing, Malden, USA, pp. 112–140.
- Ducklow, H.W., Baker, K., Martinson, D.G., Quetin, L.B., Ross, R.M., Smith, R.C., Stammerjohn, S.E., Vernet, M., Fraser, W.R., 2007. Marine pelagic ecosystems: the west Antarctic Peninsula. *Philos. T. Roy. Soc. Lon.* B362, 67–94.
- Eicken, H., 1992. The role of sea ice in structuring Antarctic ecosystems. *Polar Biol.* 12, 3–13.
- Fraser, A.D., Massom, R.A., Michael, K.J., 2010. Generation of high-resolution East Antarctic landfast sea-ice maps from cloud-free MODIS satellite composite imagery. *Remote Sens. Environ.* 114 (12), 2888–2896.
- Fraser, A.D., Massom, R.A., Michael, K.J., Galton-Fenzi, B.K., Lieser, J.L., East Antarctic sea-ice distribution and variability, 2000–2008. *J. Clim.*, Submitted for publication.
- Giles, A.B., Massom, R.A., Lytle, V.I., 2008. Fast ice distribution in East Antarctica during 1997 and 1999 determined using Radarsat data. *J. Geophys. Res.* 113, C02S14, doi:10.1029/2007JC004139.
- Gloersen, P., Campbell, W.J., Cavaleri, D.J., Comiso, J.C., Parkinson, C.L., Zwally, H.J., 1992. Arctic and Antarctic Sea Ice, 1978–1987: Satellite Passive Microwave Observations and

- Analysis (NASA SP511). National Aeronautics and Space Administration, Washington, D.C., USA.
- Greenacre, M.J., 2006. From simple to multiple correspondence analysis. In: Greenacre, M.J., Blasius, J. (Eds.), *Multiple Correspondence Analysis and Related Methods*. Chapman & Hall/CRC, Boca Raton, USA, pp. 41–76.
- Heinrichs, J.F., Cavalieri, D.J., Markus, T., 2006. Assessment of the AMSR-E sea ice concentration product at the ice edge using RADARSAT-1 and MODIS imagery. *IEEE Trans. Geosc. Rem. Sens* 55 (11), 3070–3080.
- IPCC, 2007. Summary for policymakers. Contribution of Working Group I to the Fourth Assessment Report of the Intergovernmental Panel on Climate Change. In: Solomon, S., Qin, D., Manning, M., Chen, Z., Marquis, M., Averyt, K.B., Tignor, M., Meller, H.L. (Eds.), *Climate Change 2007: The Physical Science Basis*. Cambridge University Press, Cambridge, United Kingdom and New York, NY, USA.
- Kellogg, W.W., 1975. Climatic feedback mechanisms involving the polar regions. In: Weller, G., Bowling, S.A. (Eds.), *Climate of the Arctic*. Geophysical Institute, University of Alaska, Fairbanks, pp. 111–116.
- Kusahara, K., Hasumi, H., Williams, G., 2011. Impact of the Mertz Glacier tongue calving on dense water formation and export. *Nat. Commun.* 2 doi:10.1038/ncomms1156.
- Legendre, P., Legendre, L., 1998. *Numerical Ecology*. Elsevier Science B.V., Amsterdam.
- Legrésy, B., Lescarmonier, L., Coleman, R., Young, N., Testut, L., 2010. Tidal rifting of the Mertz glacier tongue. *Geophys. Res. Abstracts* 12, EGU General Assembly 2010.
- Loeb, V., Siegel, V., Holm-Hansen, O., Hewitt, R., Fraser, W., Trivelpiece, W., Trivelpiece, S., 1997. Effect of sea-ice extent and krill or salp dominance on the Antarctic food web. *Nature* 387, 897–900.
- Loots, C., Swadling, K.M., Koubbi, P., 2009. Annual cycle of distribution of three ice-associated copepods along the coast near Dumont d'Urville, Terre Adélie (Antarctica). *J. Marine Syst.* 78, 599–605.
- Lytle, V.I., Worby, A.P., Massom, R., Paget, M.J., Allison, I., Wu, X., Roberts, A., 2001. Ice formation in the Mertz Glacier polynya, East Antarctica, during winter. *Ann. Glaciol.* 33, 368–372.
- Massom, R.A., 2003. Recent iceberg calving events in the Ninnis Glacier region, East Antarctica. *Antarct. Sci.* 15, 303–313.
- Massom, R.A., Stammerjohn, S.E., 2010. Antarctic sea ice change and variability – Physical and ecological implications. *Polar Sci.* 4 (2), 149–186.
- Massom, R.A., Harris, P.T., Michael, K.J., Potter, M.J., 1998. The distribution and formative processes of latent-heat polynyas in East Antarctica. *Ann. Glaciol.* 27, 420–426.
- Massom, R.A., Hill, K., Barbraud, C., Adams, N., Ancel, A., Emmerson, L., Pook, M., 2009. Fast ice distribution on Adélie Land, East Antarctica: Interannual variability and implications for emperor penguins *Aptenodytes forsteri*. *Mar. Ecol.-Prog. Ser.* 374, 243–257.
- Massom, R.A., Hill, K.L., Lytle, V.I., Worby, A.P., Pajet, M.J., Allison, I., 2001. Effects of regional fast-ice and iceberg distributions on the behaviour of the Mertz Glacier Polynya, East Antarctica. *Ann. Glaciol.* 33, 391–398.
- Massom, R.A., Jacka, K., Pook, M.J., Fowler, C., Adams, N., Bindoff, N., 2003. An anomalous late-season change in the regional sea ice regime in the vicinity of the Mertz Glacier Polynya, East Antarctica. *J. Geophys. Res.* 108 (5), 1–15.
- Massom, R.A., Stammerjohn, S.E., Lefebvre, W., Harangozo, S.A., Adams, N., Scambos, T.A., Pook, M.J., Fowler, C., 2008. West Antarctic Peninsula sea ice in 2005: extreme ice compaction and ice edge retreat due to strong anomaly with respect to climate. *J. Geophys. Res.* 113 doi:10.1029/2007JC004239.
- Massom, R.A., Stammerjohn, S.E., Smith, R.C., Pook, M.J., Iannuzzi, R.A., Adams, N., Martinson, D.G., Vernet, M., Fraser, W.R., Quetin, L.B., Ross, R.M., Massom, Y., Krouse, H.R., 2006. Extreme anomalous atmospheric circulation in the West Antarctic Peninsula region in Austral spring and summer 2001/02, and its profound impact on sea ice and biota. *J. Clim.* 19, 3544–3571.
- McMinn, A., Ashworth, C., Ryan, K., 2000. *In situ* net primary productivity of an Antarctic fast ice bottom algal community. *Aquat. Microb. Ecol.* 21, 177–185.
- Post, A.L., O'Brien, P.E., Beaman, R.J., Riddle, M.J., de Santis, L., 2010. Physical controls on deep water coral communities on the George V Land slope, East Antarctica. *Antarct. Sci.* 22, 371–378.
- Rintoul, S.R., 1998. On the origin and influence of Adélie Land bottom water. In: Jacobs, S.S., Weiss, R.F. (Eds.), *Ocean, Ice and Atmosphere: Interactions at the Antarctic Continental Margin*. American Geophysical Union, Washington, D.C., USA, pp. 151–172 (*Antarct. Res. Ser.* 75).
- Scambos, T., Haran, T., Fahnestock, M., Painter, T., Bohlander, J., 2007. MODIS-based mosaic of Antarctica (MOA) data sets: continent-wide surface morphology and snow grain size. *Remote Sens. Environ.* 111, 242–257.
- Scientific Community on Antarctic Research (SCAR), 2009. *Antarctic Climate Change and the Environment*. SCAR. Scott Polar Research Institute, Cambridge.
- Smith, R.C., Fraser, W.R., Stammerjohn, S.E., 2003. Climate variability and ecological response of the marine ecosystem in the western Antarctic Peninsula (WAP) region. In: Greenland, D., Goodin, D.G., Smith, R.C. (Eds.), *Climate Variability and Ecosystem Response at Long-Term Ecological Research (LTER) Sites*. Oxford University Press, New York, pp. 158–173.
- Smith, W.H.F., Sandwell, D., 1997. Global seafloor topography from satellite altimetry and ship depth soundings. *Science* 277, 1956–1962 (version 11.1 updated 2008).
- Spren, G.L., Kaleschke, L., Heygster, G., 2008. Sea ice remote sensing using AMSR-E 89 GHz channels. *J. Geophys. Res.* 113 C02S03, doi:10.1029/2005JC003384.
- Stammerjohn, S.E., Martinson, D.G., Smith, R.C., Yuan, X., Rind, D., 2008. Trends in Antarctic annual sea ice retreat and advance and their relation to El Niño–Southern Oscillation and Southern Annular Mode variability. *J. Geophys. Res.* 113 C03S90, doi:10.1029/2007JC004269.
- Tamura, T., Ohshima, K.I., Markus, T., Cavalieri, D.J., Nishishi, S., Hirasawa, N., 2007. Estimation of thin ice thickness and detection of fast ice from SSM/I data in the Antarctic ocean. *J. Atmos. Ocean. Tech.* 24, 1757–1772.
- Tamura, T., Ohshima, K.I., Nishishi, S., 2008. Mapping of sea ice production for Antarctic coastal polynyas. *Geophys. Res. Lett.* 35.
- Thomas, D.N., Dieckmann, G.S., 2010. *Sea Ice*, (Second Edition). Wiley-Blackwell, Oxford.
- Tynan, C.T., Ainley, D.G., Stirling, I., 2010. Sea ice: a critical habitat for polar marine mammals and birds. In: Thomas, D.N., Dieckmann, G.S. (Eds.), *Sea Ice*, (Second Edition). Wiley-Blackwell, Oxford, pp. 395–424.
- Vaughan, D.G., Marshall, G.J., Connelley, W.M., Parkinson, C., Mulvaney, R., Hodgson, D.A., King, J.C., Pudsey, C.J., Turner, J., 2003. Recent rapid regional climate warming on the Antarctic Peninsula. *Clim. Change* 60, 243–274.
- Wendler, G., Stearns, C., Weidner, G., Dargaud, G., Parish, T., 1997. On the extraordinary katabatic winds of Adélie Land. *J. Geophys. Res.* 102, 4463–4474, doi:10.1029/96JD03438.
- Williams, G.D., Bindoff, N.L., Marsland, S.J., Rintoul, S.R., 2008. Formation and export of dense shelf water from the Adélie

Depression, East Antarctica. *J. Geophys. Res.* 113, 4039, doi:10.1029/2007JC004346.

World Meteorological Organisation, 1970. *Sea Ice Nomenclature, Terminology, Codes, and Illustrated Glossary*. WMO/OMM/BMO 259, TP 145. Secretariat, World Meteorol. Org., Geneva.

Young, N., L egresy, B., Coleman, R., Massom, R., 2010. Mertz Glacier tongue unhinged by giant iceberg. *Aust. Antarct. Mag.* 18, 19.

Zwally, H.J., Comiso, J.C., Parkinson, C.L., Cavalieri, D.J., Gloersen, P., 2002. Variability of Antarctic sea ice 1979–1998. *J. Geophys. Res.* 107 (5), 3041, doi:10.1029/200jc000733.

